

Critical Points of Random Neural Networks

Simmaco Di Lillo

RoMaDS - Department of Mathematics, University of Rome Tor Vergata, Rome, Italy
 dilillo@mat.uniroma2.it

Abstract

This work investigates the expected number of critical points of random neural networks with different activation functions as the depth increases in the infinite-width limit. Under suitable regularity conditions, we derive precise asymptotic formulas for the expected number of critical points of fixed index and those exceeding a given threshold. Our analysis reveals three distinct regimes depending on the value of the first derivative of the covariance evaluated at 1: the expected number of critical points may converge, grow polynomially, or grow exponentially with depth. The theoretical predictions are supported by numerical experiments. Moreover, we provide numerical evidence suggesting that, when the regularity condition is not satisfied, the number of critical points increases as the map resolution increases, indicating a potential divergence in the number of critical points.

Keywords: Isotropic Gaussian Random Field, Critical Points, Deep neural networks, Kac-Rice formula, Gaussian Orthogonally Invariant Matrix.

MSCcodes: 60G60, 62B10, 62M45 .

1 Introduction

Deep architectures have consistently achieved state-of-the-art performance in applications such as image classification [26], speech recognition [24], natural language processing [38], biomedical imaging [35], clinical decision support [12] and protein structure prediction [25].

Given these practical successes, there has been a growing interest in developing a rigorous theoretical understanding of neural networks, with contributions emerging from approximation theory [6], statistical approaches [7, 36], probabilistic ones based on Gaussian processes [34] and reproducing kernel theory [2]. Alongside these developments, a growing research direction has focused on the geometric aspects of neural networks, aiming to capture the complexity of different architectures through their structural properties [31, 23, 21, 4, 9, 37]. At the same time, building on Neal’s seminal paper [33], several studies have investigated wide neural networks at initialization using the lens of Gaussian processes. It is now well established that, under random initialization and suitable scaling of the variance of weights and biases, fully-connected feedforward neural networks converge to Gaussian processes as the width of each layer tends to infinity [32, 39, 15, 27, 16, 22, 11, 5, 19, 14]. In particular, by normalizing the inputs to lie on the unit sphere, neural networks can be interpreted as random fields on the hypersphere, allowing the use of harmonic analysis and stochastic geometry to describe the underlying structure of the models. Recent studies have used this approach to analyze the angular power spectrum of such fields [17], leading to a classification of activation functions

into low-disorder, sparse, and high-disorder regimes. This classification reflects how the complexity of the network varies with depth, and has been used to explain, among other things, the observed sparsity of ReLU networks and their relative robustness to overfitting. Parallel to the analysis of the spectrum, a second line of inquiry has focused on the geometry of level and excursion sets of random neural networks. In particular, classical results from the theory of Gaussian fields, such as the Kac–Rice formula [3, 1] have been employed to compute expectations of topological invariants (e.g., Euler characteristic, Lipschitz–Killing curvatures) and to study the distribution of critical points. Such tools have been applied extensively in the context of statistical cosmology [29], and their adaptation to deep learning settings has the potential to yield novel insights into the geometric complexity of neural representations [18]. Building on these advances, the present work aims to investigate the distribution of critical points of random neural networks at initialization. More precisely, we consider neural networks with input on the d -dimensional sphere S^d and real-valued output, and we study the expected number of critical points of the limiting Gaussian field in the infinite-width regime.

Our analysis extends previous work in two main directions. First, we extend the notion of *Covariance Regularity Index* (CRI), originally introduced in [18] for CRI values below 2, which captures the smoothness of the covariance function near the diagonal. As in [18], this index determines whether classical Kac–Rice techniques can be applied, and reveals a sharp dichotomy: when the CRI exceeds 2, the field is almost surely C^2 (see Proposition 3.2), and the expected number of critical points of given index can be computed explicitly using the machinery developed in [3, 1]. In contrast, for irregular fields such as those associated with the ReLU activation, where the CRI is strictly less than 2, the classical framework breaks down. Second, we identify a simple spectral parameter that governs the asymptotic behavior of the expected number of critical points as the depth L increases (see Theorem 3.3). Depending on whether $\kappa'(1)$ is less than, equal to, or greater than one, the number of critical points exhibits qualitatively different scaling laws, corresponding respectively to vanishing, bounded, or exponentially growing complexity. This classification mirrors the one found in [17] from a spectral perspective, but it concerns a geometric quantity. We further extend our results to count critical points above a given threshold, and we derive asymptotic formulas for the expected number of such points (see Theorem 3.4). The complete proofs of the two theorems, together with some technical lemmas, are collected in Section 4

In Section 5, our theoretical findings are complemented by extensive Monte Carlo simulations using the HEALPix package [20], which confirm the predicted scaling behaviors and highlight the role of the activation function in shaping the geometric structure of the network. The empirical evidence suggests that, in irregular cases as ReLU, for instance, the number of critical points diverges, consistent with set of critical points with non-integer Hausdorff dimension

2 Background and notation

In this section we provide the necessary background and introduce the notation used throughout the paper.

2.1 Spherical random fields Let $(\Omega, \mathcal{F}, \mathbb{P})$ be a fixed probability space and let $T : \mathbb{S}^d \times \Omega \rightarrow \mathbb{R}$ be a finite-variance, zero-mean, isotropic, Gaussian random field on the d -dimensional unit sphere \mathbb{S}^d . This means that the following properties hold:

- **Measurability.** The field T is $(\mathcal{B}(\mathbb{S}^d) \otimes \mathcal{F})$ -measurable, where $\mathcal{B}(\mathbb{S}^d)$ denotes the Borel σ -algebra on \mathbb{S}^d .

- **Isotropy.** For every $g \in \text{SO}(d+1)$ (the special group of the rotations on \mathbb{R}^{d+1}), for every $k \geq 1$ and every $x_1, \dots, x_k \in \mathbb{S}^d$, the two vectors $(T(x_1), \dots, T(x_k))$ and $(T(gx_1), \dots, T(gx_k))$ have the same distribution.
- **Gaussianity.** For every $k \geq 1$ and every $x_1, \dots, x_k \in \mathbb{S}^d$, the vector $(T(x_1), \dots, T(x_k))$ is Gaussian.
- **Zero mean.** For all $x \in \mathbb{S}^d$, $\mathbb{E}[T(x)] = 0$
- **Finite variance.** For all $x \in \mathbb{S}^d$, $\text{Var}(T(x)) < \infty$

Under the previous assumption, Theorem 5.1 on [30] guarantees that the field is mean-square continuous, i.e.,

$$\lim_{x_n \rightarrow x} \mathbb{E}[|T(x_n) - T(x)|^2] = 0, \quad x \in \mathbb{S}^d,$$

and hence the following spectral decomposition holds in $L^2(\Omega \times \mathbb{S}^d)$ (see [40, Theorem 1]):

$$T(x, \omega) = \sum_{\ell \in \mathbb{N}} \sum_{m=1}^{n_{\ell,d}} a_{\ell m}(\omega) Y_{\ell m}(x), \quad x \in \mathbb{S}^d, \omega \in \Omega,$$

where $\mathbb{N} = \{0, 1, 2, \dots\}$, and

- $n_{\ell,d}$ is the number of linearly independent homogeneous harmonic polynomials of degree ℓ in $d+1$ variables given by

$$n_{0,d} = 1, \\ n_{\ell,d} = \frac{2\ell + d - 1}{\ell} \binom{\ell + d - 2}{\ell - 1}, \quad \ell \neq 0.$$

- $(a_{\ell m} \mid \ell \in \mathbb{N}, m = 1, \dots, n_{\ell,d})$ are a triangular sequence of real-valued random variables such that

$$\mathbb{E}[a_{\ell m} a_{\ell' m'}] = C_\ell \delta_{\ell, \ell'} \delta_{m, m'}$$

for a sequence $(C_\ell \mid \ell \in \mathbb{N})$, called the *angular power spectrum* of T .

- $(Y_{\ell m} \mid \ell \in \mathbb{N}, m = 1, \dots, n_{\ell,d})$ is an orthonormal sequence of spherical harmonics; i.e., each $Y_{\ell m} : \mathbb{S}^d \rightarrow \mathbb{R}$ is a harmonic homogeneous polynomial of degree ℓ in $d+1$ variables restricted to \mathbb{S}^d and

$$\int_{\mathbb{S}^d} Y_{\ell m}(x) Y_{\ell' m'}(x) \, d\text{Vol}(x) = \delta_{\ell, \ell'} \delta_{m, m'},$$

where $d\text{Vol}$ denotes the d -dimensional volume form on \mathbb{S}^d .

Let us introduce the covariance function

$$K : \mathbb{S}^d \times \mathbb{S}^d \rightarrow \mathbb{R}, \quad K(x, y) = \mathbb{E}[T(x)T(y)].$$

By isotropy, the covariance can be expressed as a function of the angle between two points, i.e., there exists $\kappa : [-1, 1] \rightarrow \mathbb{R}$ such that

$$K(x, y) = \kappa(\langle x, y \rangle),$$

where $\langle \cdot, \cdot \rangle$ denotes the scalar product in \mathbb{R}^{d+1} .

2.2 Random Neural Networks For any L , a random neural network of depth L , widths n_1, \dots, n_L , activation function $\sigma : \mathbb{R} \rightarrow \mathbb{R}$ and variance of bias equal to $\Gamma_b \in [0, 1)$ is the random field $T_L : \mathbb{S}^d \rightarrow \mathbb{R}^{n_{L+1}}$ defined in the following recursive way:

$$T_s(x) = \begin{cases} W^{(0)}x + b^{(1)}, & \text{if } s = 0, \\ W^{(s)}\sigma(T_{s-1}(x)) + b^{(s+1)}, & \text{if } s = 1, \dots, L, \end{cases} \quad x \in \mathbb{S}^d$$

where σ is applied component-wise and $(W^{(s)}, b^{(s)})$ are an independent sequence such that, for each s , $W^{(s)} \in \mathbb{R}^{n_{s+1} \times n_s}$ with $n_0 = d + 1$ and the components are i.i.d. random variables such that

$$\begin{aligned} W_{ij}^{(0)} &\sim \mathcal{N}(0, 1 - \Gamma_b) & s = 0 \\ W_{ij}^{(s)} &\sim \mathcal{N}(0, \Gamma_W n_s^{-1/2}) & s > 0 \end{aligned}$$

where

$$\Gamma_W = \frac{1 - \Gamma_b}{\mathbb{E}[\sigma(Z)^2]} \quad Z \sim \mathcal{N}(0, 1).$$

For each s , $b^{(s)} \in \mathbb{R}^{n_s}$ with i.i.d. components such that

$$b_i^{(s)} \sim \mathcal{N}(0, \Gamma_b).$$

It is well-known (see [23, 22, 8] and references therein) that the random neural network T_L converges weakly to an isotropic, zero-mean, Gaussian random field with n_{L+1} i.i.d. components as the widths n_1, \dots, n_L go to infinity. In particular, if K_L is the covariance function of one component of the limiting process, we have

$$\begin{aligned} K_L(x, y) &= \kappa_L(\langle x, y \rangle) = \underbrace{\kappa \circ \dots \circ \kappa}_{L \text{ times}}(\langle x, y \rangle) \\ \kappa(u) &= \mathbb{E} \left[\sigma(Z_1) \sigma(uZ_1 + \sqrt{1-u^2}Z_2) \right], \quad (Z_1, Z_2) \sim \mathcal{N}(0, I_2). \end{aligned} \tag{2.1}$$

We note that the condition on the variances ensures that $\kappa_L(1) = 1$ for all L and hence, for any depth, the field has unit variance.

2.3 Gaussian Orthogonally Invariant Matrix Following the notation in [28], a real symmetric random matrix $M \in \mathbb{R}^{d \times d}$ is said to be Gaussian Orthogonally Invariant (GOI) with covariance parameter c (and denoted by GOI(c)), if its entries M_{ij} are zero mean Gaussian random variables and

$$\mathbb{E}[M_{ij}M_{hk}] = \frac{1}{2}(\delta_{ih}\delta_{jk} + \delta_{ik}\delta_{jh}) + c\delta_{ij}\delta_{hk}$$

In [13] the authors derived that the density of the ordered eigenvalues of a GOI(c) matrix is given by

$$f_c(\lambda_1, \dots, \lambda_d) = \frac{\prod_{1 \leq h < k \leq d} |\lambda_h - \lambda_k|}{K_d \sqrt{1 + dc}} \exp \left(-\frac{\sum_{j=1}^d \lambda_j^2}{2} + \frac{c}{2(1 + dc)} \left(\sum_{j=1}^d \lambda_j \right)^2 \right) \mathbb{I}_{\lambda_1 \leq \dots \leq \lambda_d}, \tag{2.2}$$

where

$$K_d = 2^{d/2} \prod_{j=1}^d \Gamma(j/2).$$

is a normalization constant.

3 Main result

We extend the definition of Covariance Regularity Index given in [18].

Definition 3.1. Let T be a random field and let κ be its covariance function. We say that T has Covariance Regularity Index (CRI) equal to $\beta > 0$ if

- $\beta \in \mathbb{N}$ and $\kappa \in C^\beta([-1, 1])$
- $\beta \notin \mathbb{N}$, $\kappa \in C^{\lceil \beta \rceil}((-1, 1))$ and κ admits the following expansions around ± 1 as $t \rightarrow 0^+$

$$\begin{aligned}\kappa(1-t) &= p_1(t) + c_1 t^\beta + o(t^\beta), \\ \kappa(-1+t) &= p_{-1}(t) + c_{-1} t^\beta + o(t^\beta),\end{aligned}$$

where $\lceil \beta \rceil$ denotes the ceiling of β , p_1, p_{-1} are polynomials and c_1, c_{-1} are constants, and the first two derivatives of κ admit similar expansions obtained by differentiating the above ones.

Extending the computation of [18, Proposition 3.14] to the second derivatives, it can be shown that

Proposition 3.2. Let $T : \mathbb{S}^d \rightarrow \mathbb{R}$ be an isotropic Gaussian random field with zero mean and unit variance. If T has CRI greater than 2, then $T \in C^2(\mathbb{S}^d)$ almost surely and moreover the second derivatives are Hölder continuous.

For a given matrix A , we denote by $\text{index}(A)$ the number of its negative eigenvalues. Let $T : \mathbb{S}^d \rightarrow \mathbb{R}$ be a random field. We define

$$C_i(T) = |\{x \in \mathbb{S}^d \mid \nabla T(x) = 0, \text{index}(\nabla^2 T(x)) = i\}|$$

as the number of critical points of T with signature i , and

$$C_i(T, u) = |\{x \in \mathbb{S}^d \mid T(x) \geq u, \nabla T(x) = 0, \text{index}(\nabla^2 T(x)) = i\}|$$

as the the number of critical points of T with signature i where the field exceeds the threshold u .

Our first result provides an asymptotic formula for the expected number of critical points of a given index.

Theorem 3.3. For any L , let T_L be a random neural network with depth L . If the CRI of T_1 is greater than 2 then

$$\begin{aligned}\mathbb{E}[C_i(T_L)] &= B_i(\kappa'(1), \kappa''(1)) + o(1) && \text{if } \kappa'(1) < 1, \\ \mathbb{E}[C_i(T_L)] &= L^{d/2} \left(\frac{A_i}{\eta^{d/2}} + o(1) \right) && \text{if } \kappa'(1) = 1, \\ \mathbb{E}[C_i(T_L)] &= \kappa'(1)^{Ld/2} \left(\frac{A_i}{(\eta(\kappa'(1) - 1))^{d/2}} + o(1) \right) && \text{if } \kappa'(1) > 1\end{aligned}$$

where $\eta = \kappa'(1)/\kappa''(1)$, A_i is an absolute positive constant and B_i is a positive constant that depends only on $i, d, \kappa'(1)$ and $\kappa''(1)$.

Our second result concerns the expected number of critical points of a given index that exceed a fixed threshold $u \in \mathbb{R}$.

Theorem 3.4. Let T_L as in [Theorem 3.3](#). Then

$$\begin{aligned}\mathbb{E}[\mathcal{C}_i(T_L, u)] &= B_i(\kappa'(1), \kappa''(1))(1 - \Phi(u)) + o(1) && \text{if } \kappa'(1) < 1, \\ \mathbb{E}[\mathcal{C}_i(T_L, u)] &= L^{d/2}(A_i(1 - \Phi(u)) + o(1)) && \text{if } \kappa'(1) = 1, \\ \mathbb{E}[\mathcal{C}_i(T_L, u)] &= \kappa'(1)^{L^{d/2}}(C_i(\kappa'(1), \kappa''(1), u) + o(1)) && \text{if } \kappa'(1) > 1\end{aligned}$$

where $\Phi(u)$ is the standard Gaussian cumulative distribution function, A_i, B_i as in [Theorem 3.3](#) and C_i is another positive constant depends on $i, d, u, \kappa'(1)$ and $\kappa''(1)$.

Remark 3.5. Using the computation in [\[10\]](#), it can be shown that the CRI of a random neural networks with activation function Rectified Linear Unit (ReLU), i.e., $\sigma(x) = \max(0, x)$, is $3/2$. Consequently, the previous theoretical results are not applicable in this case. We therefore compute the number of critical points numerically. Since this number increases as the map resolution increases of the map (see [Figure 4](#) and [Table 1](#)), it is reasonable to conjecture that a ReLU network may exhibit infinitely many critical points. A possible line of investigation could involve adapting the argument used in the proof of [Theorem 3.9](#) in [\[18\]](#) to show that the set of critical points may have non-integer Hausdorff dimension. We leave a rigorous analysis of this for future work.

4 Proofs

In this section, we collect the proofs of the two theorems, but first, we need to introduce some technical lemmas regarding GOI matrices.

4.1 Technical Lemmas In this section, we collect three auxiliary results which will be used in the proof of our main results. To simplify the proof we make use of the following notation

- $\boldsymbol{\lambda}$ is a vector in \mathbb{R}^d with $\lambda_1, \dots, \lambda_d$ as components. Analogously for other bold letters.
- $\mathbf{1}$ is the vector in \mathbb{R}^d with all components equal to 1.
- If $\boldsymbol{v}, \boldsymbol{w} \in \mathbb{R}^d$, $\boldsymbol{v}\boldsymbol{w}^\top$ denotes the matrix $M \in \mathbb{R}^{d \times d}$ with entries $M_{ij} = v_i w_j$.
- For a function $g : \mathbb{R}^d \rightarrow \mathbb{R}$, the symbol $\mathbb{E}_{\text{GOI}(c)}^d[g(\boldsymbol{\lambda})]$ is just a way to write

$$\int_{\mathbb{R}^d} g(\boldsymbol{\lambda}) f_c(\boldsymbol{\lambda}) d\boldsymbol{\lambda} \tag{4.1}$$

where f_c is the density of ordered eigenvalues of a $\text{GOI}(c)$ matrix given by [\(4.2\)](#).

- Let

$$\mathcal{O} = \left\{ \boldsymbol{x} \in \mathbb{R}^d \mid x_i \leq x_{i+1} \ i = 1, \dots, d-1 \right\}$$

be the subsets of \mathbb{R}^d consisting of all vectors with non-decreasing components and for any $i = 0, \dots, d$, let \mathcal{O}_i be the subset of \mathbb{R}^d given by

$$\begin{aligned}\mathcal{O}_0 &= \left\{ \boldsymbol{x} \in \mathbb{R}^d \mid 0 < x_1 \right\}, \\ \mathcal{O}_i &= \left\{ \boldsymbol{x} \in \mathbb{R}^d \mid x_i < 0 < x_{i+1} \right\}, \quad i = 1, \dots, d-1, \\ \mathcal{O}_d &= \left\{ \boldsymbol{x} \in \mathbb{R}^d \mid x_d < 0 \right\}.\end{aligned}$$

- For any set $A \subseteq \mathbb{R}^d$ let \mathbb{I}_A denotes its indicator function, i.e.

$$\mathbb{I}_A(\mathbf{x}) = \begin{cases} 1 & \text{if } \mathbf{x} \in A \\ 0 & \text{otherwise} \end{cases}.$$

- Let $\Delta : \mathbb{R}^d \rightarrow \mathbb{R}$ be the function given by

$$\Delta(\mathbf{x}) = \prod_{1 \leq i < j \leq d} |x_i - x_j|.$$

- Let $\Pi : \mathbb{R}^d \rightarrow \mathbb{R}$ be the function given by

$$\Pi(\mathbf{x}) = \prod_{i=1}^d |x_i|.$$

We note that using the previous notations, one can write the density f_c in a compact way:

$$f_c(\boldsymbol{\lambda}) = \frac{1}{K_d \sqrt{1+dc}} \exp\left(-\frac{\|\boldsymbol{\lambda}\|^2}{2} + \frac{c(\mathbf{1}^\top \boldsymbol{\lambda})^2}{2(1+dc)}\right) \Delta(\boldsymbol{\lambda}) \mathbb{I}_{\mathcal{O}}(\boldsymbol{\lambda}) \quad (4.2)$$

Lemma 4.1. *Let (c_n) be a sequence of number and let $a_n = \frac{1+c_n}{2}$. If $c_n \rightarrow c$ then*

$$\lim_{n \rightarrow \infty} \mathbb{E}_{\text{GOI}(a_n)}^d [\Pi(\boldsymbol{\lambda}) \mathbb{I}_{\mathcal{O}_i}(\boldsymbol{\lambda})] = \mathbb{E}_{\text{GOI}(\frac{1+c}{2})}^d [\Pi(\boldsymbol{\lambda}) \mathbb{I}_{\mathcal{O}_i}(\boldsymbol{\lambda})].$$

Proof. Since the the density of the ordered eigenvalues of a $\text{GOI}(a)$ matrix is a function continuous in a , for all $\boldsymbol{\lambda} \in \mathbb{R}^d$ we have

$$\lim_{n \rightarrow \infty} f_{a_n}(\boldsymbol{\lambda}) \Pi(\boldsymbol{\lambda}) \mathbb{I}_{\mathcal{O}_i}(\boldsymbol{\lambda}) = f_{\frac{1+c}{2}}(\boldsymbol{\lambda}) \Pi(\boldsymbol{\lambda}) \mathbb{I}_{\mathcal{O}_i}(\boldsymbol{\lambda}).$$

We now show that this pointwise convergence is dominated by an integrable function. We observe that

$$\lim_{n \rightarrow \infty} a_n = \frac{1+c}{2}$$

and

$$\lim_{n \rightarrow \infty} \frac{a_n}{2(1+da_n)} = \lim_{n \rightarrow \infty} \frac{1+c_n}{2(2+d(1+c_n))} = \frac{1+c}{2(2+d(1+c))}.$$

Therefore, for every $\varepsilon > 0$, there exists an integer n_ε such that for all $n \geq n_\varepsilon$, the following inequalities hold:

$$\begin{aligned} \frac{1}{\sqrt{1+da_n}} &\leq \sqrt{\frac{2}{2+d(1+c)}} + \varepsilon, \\ \frac{a_n}{2(1+da_n)} &\leq \frac{1+c}{2(2+d(1+c))} + \varepsilon^2. \end{aligned}$$

In particular, choosing $\varepsilon = (2d(2+d(1+c)))^{-1/2}$, we obtain that definitely in n ,

$$\begin{aligned} \frac{a_n}{2(1+da_n)} &\leq \frac{d+cd+1}{2d(2+d(1+c))}, \\ \frac{1}{\sqrt{1+da_n}} &\leq \frac{2\sqrt{d}+1}{\sqrt{2(2+d(1+c))}}. \end{aligned}$$

Putting $C_{d;c} = \frac{2\sqrt{d}+1}{\sqrt{2+d(1+c)2^{(d+1)/2}}}$ we have

$$\begin{aligned} f_{a_n}(\boldsymbol{\lambda})\Pi(\boldsymbol{\lambda})\mathbb{I}_{\mathcal{O}_i}(\boldsymbol{\lambda}) &\leq C_{d;c} \exp\left(-\frac{\|\boldsymbol{\lambda}\|^2}{2} + \frac{d+cd+1}{2d(2+d(1+c))}(\mathbf{1}^\top \boldsymbol{\lambda})^2\right) \Pi(\boldsymbol{\lambda})\Delta(\boldsymbol{\lambda})\mathbb{I}_{\mathcal{O}_i \cap \mathcal{O}}(\boldsymbol{\lambda}) \\ &\leq C_{d;c} \exp\left(-\frac{1}{2}\left(1 - \frac{d+cd+1}{2+d(1+c)}\right)\|\boldsymbol{\lambda}\|^2\right) \Pi(\boldsymbol{\lambda})\Delta(\boldsymbol{\lambda})\mathbb{I}_{\mathcal{O}_i \cap \mathcal{O}}(\boldsymbol{\lambda}) \\ &= C_{d;c} \exp\left(-\frac{\|\boldsymbol{\lambda}\|^2}{2+d(1+c)}\right) \Pi(\boldsymbol{\lambda})\Delta(\boldsymbol{\lambda})\mathbb{I}_{\mathcal{O}_i \cap \mathcal{O}}(\boldsymbol{\lambda}) \end{aligned}$$

where the second inequality follows from the Cauchy-Schwarz inequality. Let $g(\boldsymbol{\lambda})$ denote the right-hand side of the last equality and letting

$$D_{c;d} = C_{d;c}(2\pi(2+d(1+c)))^{d/2}.$$

If $\tilde{\boldsymbol{Z}} \sim \mathcal{N}(0, (2+d(1+c))I_d)$ we obtain

$$\begin{aligned} \int_{\mathbb{R}^d} g(\boldsymbol{\lambda}) \, d\boldsymbol{\lambda} &= D_{c;d} \mathbb{E} \left[\Pi(\tilde{\boldsymbol{Z}})\Delta(\tilde{\boldsymbol{Z}})\mathbb{I}_{\mathcal{O}_i \cap \mathcal{O}}(\tilde{\boldsymbol{Z}}) \right] \\ &\leq D_{c;d}(2+d(1+c))^{(d^2+d)/2} \mathbb{E} [\Pi(\boldsymbol{Z})\Delta(\boldsymbol{Z})\mathbb{I}_{\mathcal{O}_i \cap \mathcal{O}}(\boldsymbol{Z})] \\ &\leq D_{c;d}(2+d(1+c))^{(d^2+d)/2} \mathbb{E} [\Pi(\boldsymbol{Z})\Delta(\boldsymbol{Z})\mathbb{I}_{\mathcal{O}}(\boldsymbol{Z})] \end{aligned} \tag{4.3}$$

where $\boldsymbol{Z} \sim \mathcal{N}(0, I_d)$ and we have used the identities

$$\begin{aligned} \Pi(a\boldsymbol{x}) &= a^d \Pi(\boldsymbol{x}), \\ \Delta(a\boldsymbol{x}) &= a^{(d^2-d)/2} \Delta(\boldsymbol{x}). \end{aligned}$$

To bound the previous quantity, one can observe that

$$|Z_j| \mathbb{I}_{\mathcal{O}}(\boldsymbol{Z}) \leq \max\{|Z_1|, |Z_d|\}.$$

Hence

$$\Pi(\boldsymbol{Z})\mathbb{I}_{\mathcal{O}}(\boldsymbol{Z}) \leq \max\{|Z_1|, |Z_d|\}^d$$

and

$$\Delta(\boldsymbol{Z})\mathbb{I}_{\mathcal{O}}(\boldsymbol{Z}) \leq 2^{(d^2-d)/2} \max\{|Z_1|, |Z_d|\}^{(d^2-d)/2}. \tag{4.4}$$

Therefore, using (4.3), we obtain

$$\begin{aligned} \int_{\mathbb{R}^d} g(\boldsymbol{\lambda}) \, d\boldsymbol{\lambda} &\leq 2^{(d^2-d)/2} D_{c;d}(2+d(1+c))^{(d^2+d)/2} \mathbb{E} \left[\max\{|Z_1|, |Z_d|\}^{(d^2+d)/2} \right] \\ &\leq 2^{d^2} D_{c;d}(2+d(1+c))^{(d^2+d)/2} \mathbb{E} \left[|Z_1|^{(d^2+d)/2} \right] < \infty \end{aligned}$$

where the last inequality follows since a Gaussian random variable has all absolute moments finite. One can conclude using the dominated convergence theorem. \square

The next lemma provides an explicit change of variables that transforms the integrand into a function of a Gaussian vector with a suitable covariance matrix. As a consequence, one can estimate the original integral by generating samples from a multivariate Gaussian distribution and applying a Monte Carlo method. This lemma also allows us to numerically approximate with respect to a GOI distribution. Instead of sampling from the GOI distribution directly we can sample a standard Gaussian vector with a known covariance structure and compute the corresponding average of the transformed integrand (see [Section 5](#) for more details)

Lemma 4.2. Let $c \geq -\frac{1}{d}$ then

$$\mathbb{E}_{\text{GOI}(c)}^d [g(\boldsymbol{\lambda})] = \frac{(2\pi)^{d/2}}{K_d} \mathbb{E} [g(\mathbf{Z})\Delta(\mathbf{Z})\mathbb{I}_{\mathcal{O}}(\mathbf{Z})]$$

where $\mathbf{Z} \sim \mathcal{N}(0, \Gamma_{c;d})$ with $\Gamma_{c;d} = I_d + c\mathbf{1}\mathbf{1}^\top$.

Proof. From (4.2) we obtain

$$f_c(\boldsymbol{\lambda}) = \frac{1}{K_d \sqrt{1+dc}} \exp \left(-\frac{1}{2} \left(\frac{1+dc-c}{1+dc} \|\boldsymbol{\lambda}\|^2 - 2 \sum_{1 \leq h < k \leq d} \frac{c}{1+dc} \lambda_h \lambda_k \right) \right) \Delta(\boldsymbol{\lambda}) \mathbb{I}_{\mathcal{O}}(\boldsymbol{\lambda}).$$

If we put

$$A_{c;d} = I_d - \frac{c}{1+dc} \mathbf{1}\mathbf{1}^\top$$

then

$$f_c(\boldsymbol{\lambda}) = \frac{1}{K_d \sqrt{1+dc}} \exp \left(-\frac{1}{2} \boldsymbol{\lambda}^\top A_{c;d} \boldsymbol{\lambda} \right) \Delta(\boldsymbol{\lambda}) \mathbb{I}_{\mathcal{O}}(\boldsymbol{\lambda}). \quad (4.5)$$

We note that for every $\mathbf{x} \in \mathbb{R}^d$

$$\begin{aligned} A_{c;d} \Gamma_{c;d} \mathbf{x} &= \left(I_d - \frac{c}{1+dc} \mathbf{1}\mathbf{1}^\top \right) (I_d + c\mathbf{1}\mathbf{1}^\top) \mathbf{x} = \left(I_d - \frac{c}{1+dc} \mathbf{1}\mathbf{1}^\top \right) (\mathbf{x} + c(\mathbf{1}^\top \mathbf{x}) \mathbf{1}) \\ &= \mathbf{x} + \left(c - \frac{c}{1+dc} - \frac{c^2(\mathbf{1}^\top \mathbf{1})}{1+dc} \right) (\mathbf{1}^\top \mathbf{x}) \mathbf{1} = \mathbf{x} \end{aligned}$$

where the last equality follows from the identity $\mathbf{1}^\top \mathbf{1} = d$. Since this holds for arbitrary \mathbf{x} , we conclude that $\Gamma_{c;d} = A_{c;d}^{-1}$. In particular, since $A_{c;d}$ is symmetric, it follows that $\Gamma_{c;d}$ is symmetric as well.

Let us compute the eigenpairs of $\Gamma_{c;d}$. Let $\mathbf{v}_1, \dots, \mathbf{v}_{d-1}$ be a basis of $\text{Span}(\mathbf{1})^\perp$ then

$$\Gamma_{c;d} \mathbf{v}_i = \mathbf{v}_i, \quad i = 1, \dots, d-1$$

and

$$\Gamma_{c;d} \mathbf{1} = \mathbf{1} + c(\mathbf{1}^\top \mathbf{1}) \mathbf{1} = (1+dc) \mathbf{1}.$$

We have thus shown that 1 is an eigenvalue of $\Gamma_{c;d}$ with geometric multiplicity $d-1$, and that $1+dc$ is a simple eigenvalue. In particular, $\Gamma_{c;d}$ has positive eigenvalue and thus it is positive definite. Recalling that the density of a centered Gaussian vector with covariance matrix $A \in \mathbb{R}^{d \times d}$ is given by

$$f_A(\mathbf{x}) = \frac{1}{(2\pi)^{d/2} \sqrt{\det(A)}} \exp \left(-\frac{1}{2} \mathbf{x}^\top A \mathbf{x} \right),$$

we can rewrite (4.5) as

$$f_c(\boldsymbol{\lambda}) = \Delta(\boldsymbol{\lambda}) \mathbb{I}_{\mathcal{O}}(\boldsymbol{\lambda}) \frac{(2\pi)^{d/2}}{K_d} f_{\Gamma_{c;d}}(\boldsymbol{\lambda})$$

and hence the claim. \square

Before stating the next lemma, we introduce the following notation. If $\xi, x \in \mathbb{R}$ and $\boldsymbol{\lambda} \in \mathbb{R}^d$, we denote by $\boldsymbol{\lambda}_{\xi, x}$ the vector whose components are given by $\lambda_i - \frac{\xi x}{\sqrt{2}}$ for $i = 1, \dots, d$.

Lemma 4.3. Let $c > -1/d$ and let $\xi_L \rightarrow \xi$. Then for every u

$$\lim_{L \rightarrow +\infty} \int_u^\infty \phi(x) \mathbb{E}_{\text{GOI}(c)}^d [\Pi(\boldsymbol{\lambda}_{\xi_L, x}) \mathbb{I}_{\mathcal{O}_i}(\boldsymbol{\lambda}_{\xi_L, x})] dx = \int_u^\infty \phi(x) \mathbb{E}_{\text{GOI}(c)}^d [\Pi(\boldsymbol{\lambda}_{\xi, x}) \mathbb{I}_{\mathcal{O}_i}(\boldsymbol{\lambda}_{\xi, x})] dx$$

where ϕ is the standard normal density function.

Proof. Let $\mathbf{Z} \sim \mathcal{N}(0, \Gamma_{c;d})$ where $\Gamma_{c;d}$ is as in Lemma 4.2. If we put $C = (2\pi)^{d/2} K_d^{-1}$ then

$$\begin{aligned} & \int_u^\infty \phi(x) \mathbb{E}_{\text{GOI}(c)}^d [\Pi(\boldsymbol{\lambda}_{\xi_L, x}) \mathbb{I}_{\mathcal{O}_i}(\boldsymbol{\lambda}_{\xi_L, x})] dx \\ &= C \int_u^\infty \phi(x) \mathbb{E}_{\mathbf{Z}} [\Pi(\mathbf{Z}_{\xi_L, x}) \mathbb{I}_{\mathcal{O}_i}(\mathbf{Z}_{\xi_L, x}) \Delta(\mathbf{Z}) \mathbb{I}_{\mathcal{O}}(\mathbf{Z})] dx \\ &= \frac{C}{(2\pi)^{d/2} \sqrt{1+dc}} \int_u^\infty \int_{\mathbb{R}^d} \phi(x) \Pi(\boldsymbol{\lambda}_{\xi_L, x}) \mathbb{I}_{\mathcal{O}_i}(\boldsymbol{\lambda}_{\xi_L, x}) \Delta(\boldsymbol{\lambda}) \mathbb{I}_{\mathcal{O}}(\boldsymbol{\lambda}) f_{\Gamma_{c;d}}(\boldsymbol{\lambda}) d\boldsymbol{\lambda} dx. \end{aligned}$$

Let

$$g_L(\boldsymbol{\lambda}, x) = \phi(x) \Pi(\boldsymbol{\lambda}_{\xi_L, x}) \mathbb{I}_{\mathcal{O}_i}(\boldsymbol{\lambda}_{\xi_L, x}) \Delta(\boldsymbol{\lambda}) \mathbb{I}_{\mathcal{O}}(\boldsymbol{\lambda}) f_{\Gamma_{c;d}}(\boldsymbol{\lambda})$$

We note that if $\mathbb{I}_{\mathcal{O}}(\boldsymbol{\lambda}) \mathbb{I}_{\mathcal{O}_i}(\boldsymbol{\lambda}_{\xi_L, x}) \neq 0$ then

$$\Pi(\boldsymbol{\lambda}_{\xi_L, x}) \leq \max \left\{ \left| \lambda_1 - \frac{\xi_L x}{\sqrt{2}} \right|, \left| \lambda_d - \frac{\xi_L x}{\sqrt{2}} \right| \right\}$$

and

$$\begin{aligned} \Pi(\boldsymbol{\lambda}_{\xi_L, x}) &\leq \max \left\{ \left| \lambda_1 - \frac{\xi_L x}{\sqrt{2}} \right|, \left| \lambda_d - \frac{\xi_L x}{\sqrt{2}} \right| \right\}^d \\ &\leq \left| \lambda_1 - \frac{\xi_L x}{\sqrt{2}} \right|^d + \left| \lambda_d - \frac{\xi_L x}{\sqrt{2}} \right|^d \\ &\leq 2^d \left(|\lambda_1|^d + |\lambda_d|^d + 2^{1-d/2} |\xi_L x|^d \right) \end{aligned} \tag{4.6}$$

where in the last inequality we used that, for all $a, b \in \mathbb{R}$, it holds that

$$|a - b|^d \leq 2^d (|a|^d + |b|^d).$$

Now, since $\xi_n x \rightarrow \xi x$, we have $\xi_n x \leq \xi x + 2^{-d} \varepsilon^{1/d}$ for n large enough. Hence

$$|\xi_n x|^d \leq 2^d \left(|\xi x|^d + 2^{-d} \varepsilon \right)$$

and thus, from equation (4.6), we obtain

$$\Pi(\boldsymbol{\lambda}_{\xi_L, x}) \leq 2^d \left(|\lambda_1|^d + |\lambda_d|^d + 2^{(d+2)/2} |\xi x|^d + \varepsilon \right).$$

Combining the previous inequality with (4.4), it follows that

$$\begin{aligned} & g_L(\boldsymbol{\lambda}, x) \\ &\leq \phi(x) 2^{(d^2+d)/2} \left(|\lambda_1|^d + |\lambda_d|^d + 2^{(d+2)/2} |\xi x|^d + \varepsilon \right) \left(|\lambda_1|^{(d^2-d)/2} + |\lambda_d|^{(d^2-d)/2} \right) f_{\Gamma_{c;d}}(\boldsymbol{\lambda}) \\ &= \phi(x) 2^{(d^2+d)/2} \left(|\lambda_1|^d + |\lambda_d|^d + \varepsilon \right) \left(|\lambda_1|^{(d^2-d)/2} + |\lambda_d|^{(d^2-d)/2} \right) f_{\Gamma_{c;d}}(\boldsymbol{\lambda}) \\ &\quad + 2^{(d^2+2d+2)/2} |\xi x|^d \left(|\lambda_1|^{(d^2-d)/2} + |\lambda_d|^{(d^2-d)/2} \right) f_{\Gamma_{c;d}}(\boldsymbol{\lambda}). \end{aligned}$$

So, if we denote by $\phi(x)h_1(\boldsymbol{\lambda})$ the expression on the second-to-last line, and by $h_2(\boldsymbol{\lambda})\phi(x)|x|^d$ the expression on the last line, then we have

$$g_L(\boldsymbol{\lambda}, x) \leq h_1(\boldsymbol{\lambda})\phi(x) + h_2(\boldsymbol{\lambda}, x)\phi(x)|x|^d$$

and recalling the definition of $\Gamma_{c;d}$ we have

$$\begin{aligned} & \int_u^\infty \int_{\mathbb{R}^d} (h_1(\boldsymbol{\lambda})\phi(x) + h_2(\boldsymbol{\lambda}, x)\phi(x)|x|^d) d\boldsymbol{\lambda} dx \\ &= 2(1 - \Phi(u))\mathbb{E} \left[|Z_1|^{(d^2+d)/2} + |Z_1|^d |Z_2|^{(d^2-d)/2} + \varepsilon |Z_1|^{(d^2-d)/2} \right] \\ & \quad + 2\mathbb{E} \left[|Z|^d \mathbb{I}_{[u, +\infty)}(Z) \right] \mathbb{E}[|Z_1|^{(d^2-d)/2}] \end{aligned}$$

for $Z \sim \mathcal{N}(0, 1)$ and Z_1, Z_2 zero-mean Gaussian random variable with variance $1+c$ and covariance equal to c . The claim follows by dominated convergence. \square

4.2 Proof of Theorem 3.3 Since the CRI of T_L is greater than 2 the second derivatives of T_L are Höldercontinuous and so

- i) the gradient and Hessian exist in an almost sure sense and their joint distribution are not degenerate,
- ii) for some constant K and α , uniformly in t ,

$$\max_{i,j} \mathbb{E} \left[(E_{ij}T_L(t) - E_{ij}T_L(s))^2 \right] \leq K |\ln |t - s||^{-(1+\alpha)}. \quad (4.7)$$

where $(E_i \mid i = 1, \dots, d)$ is an orthonormal frame of \mathbb{S}^d .

Hence the sample functions of T are, with probability one, Morse function and one can apply the Adler-Taylor Expectation Metatheorem and the Crofton's formula (see [1] for more details). So using the results in [13] we have

$$\mathbb{E}[\mathcal{C}_i(T_L)] = \frac{2\sqrt{\pi}}{\Gamma\left(\frac{d+1}{2}\right)\eta_L^{d/2}} \mathbb{E}_{\text{GOI}\left(\frac{1+\eta_L}{2}\right)}^d [\Pi(\boldsymbol{\lambda})\mathbb{I}_{\mathcal{O}_i}(\boldsymbol{\lambda})] \quad (4.8)$$

where $\eta_L = \kappa'_L(1)(\kappa''_L(1))^{-1}$. In order to obtain a closed formula for η_L , we use the computation in [17]:

$$\kappa'_L(1) = \kappa'(1)^L \quad (4.9)$$

and

$$\kappa''_L(1) = \begin{cases} L\kappa''(1) & \text{if } \kappa'(1) = 1 \\ \kappa''(1)\kappa'(1)^{L-1} \frac{\kappa'(1)^{L-1}}{\kappa'(1)-1} & \text{if } \kappa'(1) \neq 1 \end{cases}. \quad (4.10)$$

Therefore,

$$\begin{aligned} \eta_L &= \eta_1(1 - \kappa'(1)) + o(1) && \text{if } \kappa'(1) < 1, \\ \eta_L &= L^{-1}\eta_1 && \text{if } \kappa'(1) = 1, \\ \eta_L &= \kappa'(1)^{-L} (\eta_1(\kappa'(1) - 1) + o(1)) && \text{if } \kappa'(1) > 1. \end{aligned}$$

Now, if $\kappa'(1) \geq 1$ then $\eta_L \rightarrow 0$ so using [Lemma 4.1](#) we have,

$$\lim_{L \rightarrow \infty} \mathbb{E}_{\text{GOI}\left(\frac{1+\eta_L}{2}\right)}^d [\Pi(\boldsymbol{\lambda}) \mathbb{I}_{\mathcal{O}_i}(\boldsymbol{\lambda})] = \mathbb{E}_{\text{GOI}\left(\frac{1}{2}\right)}^d [\Pi(\boldsymbol{\lambda}) \mathbb{I}_{\mathcal{O}_i}(\boldsymbol{\lambda})].$$

Otherwise, if $\kappa'(1) < 1$ then $1 + \eta_L \rightarrow 1 + \eta_1(1 - \kappa'(1))$. Using, [Lemma 4.1](#) again, we have

$$\mathbb{E}_{\text{GOI}\left(\frac{1+\eta_L}{2}\right)}^d [\Pi(\boldsymbol{\lambda}) \mathbb{I}_{\mathcal{O}_i}(\boldsymbol{\lambda})] \rightarrow \mathbb{E}_{\text{GOI}\left(\frac{1+\eta_1(1-\kappa'(1))}{2}\right)}^d [\Pi(\boldsymbol{\lambda}) \mathbb{I}_{\mathcal{O}_i}(\boldsymbol{\lambda})].$$

The result then follows from [Lemma 4.2](#).

4.3 Proof of [Theorem 3.4](#) Using the observation in the previous section, we can apply the Kac-Rice formula and, in particular, the results in [\[13\]](#). Hence

$$\mathbb{E}[\mathcal{C}_i(T_L, u)] = \frac{2\sqrt{\pi}}{\Gamma\left(\frac{d+1}{2}\right) \eta_L^{d/2}} \int_u^{+\infty} \phi(x) \mathbb{E}_{\text{GOI}\left(\frac{1+\eta_L-\xi_L}{2}\right)} [\Pi(\boldsymbol{\lambda}_{\xi_L, x}) \mathbb{I}_{\mathcal{O}_i}(\boldsymbol{\lambda}_{\xi_L, x})] dx$$

where η_L is as above and $\xi_L = \kappa'_L(1)^2(\kappa''_L(1))^{-1}$. So, using [\(4.9\)](#) and [\(4.10\)](#) we have

$$\begin{aligned} \xi_L &= L^{-1} \eta_1 && \text{if } \kappa'(1) = 1 \\ \xi_L &= \eta_1(\kappa'(1) - 1) + o(1) && \text{if } \kappa'(1) > 1 \\ \xi_L &= \kappa'(1)^L (\eta_1(1 - \kappa'(1)) + o(1)) && \text{if } \kappa'(1) < 1 \end{aligned}$$

and

$$\begin{aligned} \frac{1 + \eta_L - \xi_L}{2} &= \frac{1}{2} && \text{if } \kappa'(1) = 1 \\ \frac{1 + \eta_L - \xi_L}{2} &= \frac{1}{2}(1 + \eta_1(1 - \kappa'(1))) = c && \text{if } \kappa'(1) \neq 1. \end{aligned}$$

The claim follows using [Lemma 4.3](#).

5 Numerical Evidences

In this section, we will present a series of numerical experiments designed to provide empirical support for the theoretical results established in the preceding sections. These experiments are crucial as they offer insights into the practical applicability of our theoretical findings and help validate the underlying models.

All the experiments conducted can be easily reproduced by cloning the corresponding GitHub repository: <https://github.com/simmaco99/SpectralComplexity>. All the simulations are conducted on \mathbb{S}^2 using the Healpix package [\[20\]](#), which is widely recognized for its capabilities in handling pixelization of the sphere and performing analyses in spherical harmonics.

To validate the results of [Theorem 3.3](#), we follow the approach of [\[18\]](#) and use the Gaussian activation function defined by $\sigma_a(u) = e^{-\frac{a}{2}u^2}$, considering three different values for the parameter a . This choice allows us to explore all three regimes: for the low-disorder case, we set $a = 1$; for the sparse case, we take $a = 1 + \sqrt{2}$; and for the high-disorder case, we choose $a = 3$. To compute numerically the expected number of minima and maxima, for each value of a , we generate 1000 random neural networks with input on \mathbb{S}^2 and hidden layers of width $n = 1000$. [Figure 1](#)

shows the Monte Carlo estimation of the number of minima and maxima. To obtain the theoretical values, one must know the value of A_0 ; we use [Lemma 4.2](#) to express it as an expectation over Gaussian variables, which we estimate using a Monte Carlo method. In [Figure 2](#), we illustrate how the estimated value of A_0 changes as the number of samples increases. In [Figure 1\(c\)](#), we observe that the theoretical and estimated values closely match as long as the depth remains below $L = 40$. This is due to the fact that, working in finite-precision arithmetic, all our random fields are truncated at frequency $\ell_{\max} = 1356$, and therefore we inevitably lose information for sufficiently large L . This loss is confirmed by [Figure 3](#), where we compute the percentage of variance explained using only the first 1356 frequencies. We note that this percentage starts to decrease precisely from $L = 40$ onward.

Since the results of [Theorem 3.3](#) cannot be applied to irregular fields (such as fields generated by ReLU activation), [Figure 4](#) and [Table 1](#) shows how for a ReLU network the number of critical points increases with the resolution of the map (suggesting a potential divergence, as noted in [Remark 3.5](#)), while it remains approximately constant in the case of fields associated with more regular activation (as σ_1 or tanh).

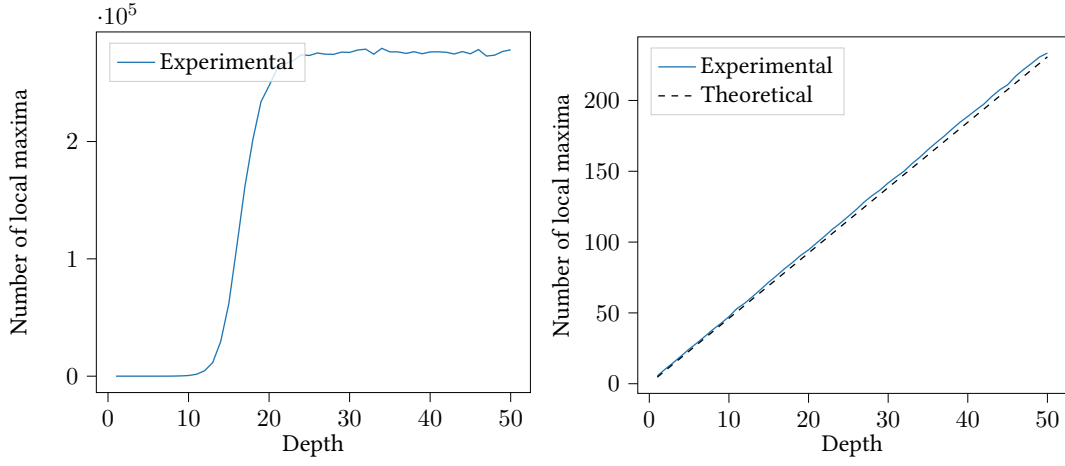
Table 1: Number of local minima and maxima for different activations and number of pixels. A resolution level r corresponds to a HEALPix map with $12 \cdot 2^{2r}$ pixels.

(a) Local minima

Resolution	Gaussian	ReLU	tanh
3	3.108	3.085	1.548
4	3.136	5.367	1.569
5	3.260	9.900	1.563
6	3.182	18.10	1.620
7	3.146	31.28	1.661
8	3.176	53.51	1.677
9	4.750	93.40	1.570

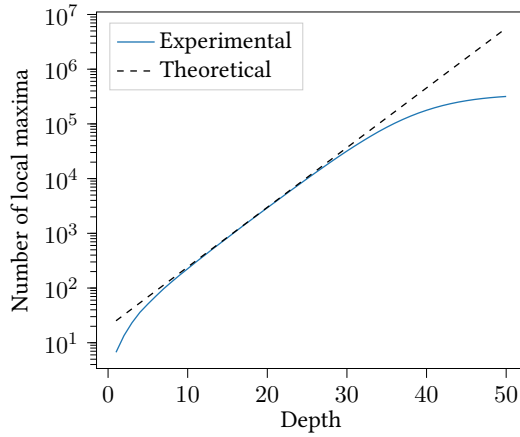
(b) Local maxima

Resolution	Gaussian	ReLU	tanh
3	3.082	3.027	1.552
4	3.094	5.313	1.570
5	3.174	9.710	1.563
6	3.270	18.17	1.619
7	3.102	31.80	1.661
8	3.150	53.49	1.677
9	4.820	93.48	1.575



(a) Low-disorder case: $a = 1$

(b) Sparse case: $a = 1 + \sqrt{2}$



(c) High-disorder case: $a = 3$

Figure 1: Number of minima and maxima points for the Gaussian activation function with different values of a . The dashed lines are the theoretical behaviour without multiplicative constant independent from L . These numbers are computed using 1000 Monte Carlo replicas.

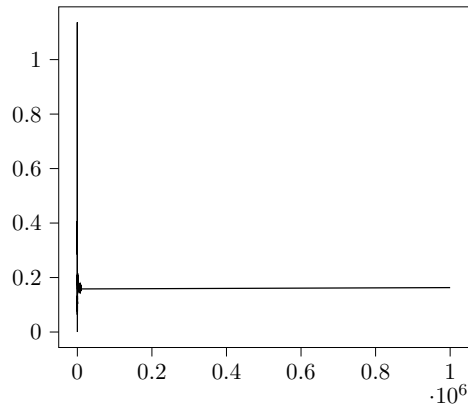


Figure 2: Approximation of the A_0 as the number of Monte Carlo replicas increases. The figure shows the value for $d = 2$ up to the volume of the sphere \mathbb{S}^d .

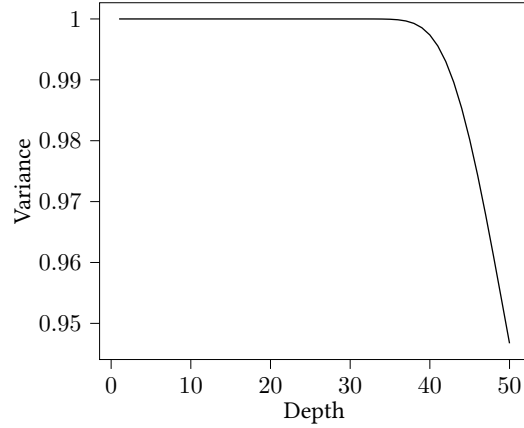


Figure 3: Percentage of the variance explained by using the first 1536 frequencies for random neural networks on \mathbb{S}^2 with σ_3 as activation function for different values of depth L . To obtain the plot, we compute the angular power spectrum of this network using a Gauss-Legendre quadrature with 5000 points.

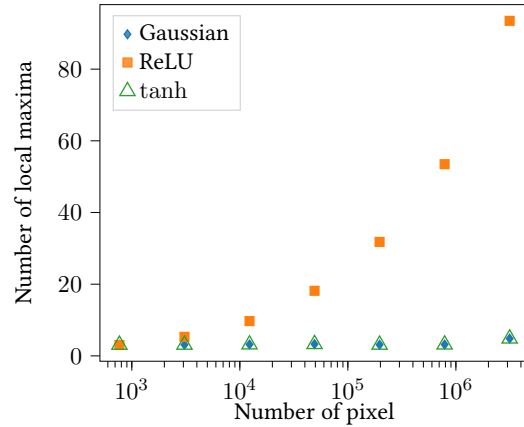


Figure 4: Mean of the number of local maxima in 1000 Monte Carlo replica. The fields are shallow (one hidden layer) random neural network with 1000 neurons. In the simulation we can use three different activation function: Gaussian with $a = 1 + \sqrt{2}$ (diamond), ReLU (square) and tanh (triangle).

Acknowledgements The author wishes to thank Professor Domenico Marinucci for his helpful suggestions and insightful discussions.

This work was partially supported by the MUR Excellence Department Project MatMod@TOV awarded to the Department of Mathematics, University of Rome Tor Vergata, CUP E83C18000100006. We also acknowledge financial support from the MUR 2022 PRIN project GRAFIA, project code 202284Z9E4.

The author is member of the Gruppo Nazionale per l'Analisi Matematica, la Probabilità e le loro Applicazioni (GNAMPA), which is part of the Istituto Nazionale di Alta Matematica (INdAM).

References

- [1] Robert J. Adler and Jonathan E. Taylor. *Random fields and geometry*. Springer Monographs in Mathematics. Springer, New York, 2007.
- [2] N. Aronszajn. Theory of Reproducing Kernels. *Transactions of the American Mathematical Society*, 68(3):337–404, 1950.
- [3] Jean-Marc Azaïs and Mario Wschebor. *Level sets and extrema of random processes and fields*. John Wiley & Sons, Inc., Hoboken, NJ, 2009.
- [4] Shayan Aziznejad, Joaquim Campos, and Michael Unser. Measuring complexity of learning schemes using Hessian-Schatten total variation. *SIAM J. Math. Data Sci.*, 5(2):422–445, 2023.
- [5] Krishnakumar Balasubramanian, Larry Goldstein, Nathan Ross, and Adil Salim. Gaussian random field approximation via stein’s method with applications to wide random neural networks. *Applied and Computational Harmonic Analysis*, 72:101668, 2024.
- [6] Peter L. Bartlett, Andrea Montanari, and Alexander Rakhlin. Deep learning: a statistical viewpoint. *Acta Numer.*, 30:87–201, 2021.
- [7] Peter L. Bartlett, Andrea Montanari, and Alexander Rakhlin. Deep learning: a statistical viewpoint. *Acta Numer.*, 30:87–201, 2021.
- [8] Andrea Basteri and Dario Trevisan. Quantitative Gaussian approximation of randomly initialized deep neural networks. *Mach. Learn.*, 113(9):6373–6393, 2024.
- [9] Monica Bianchini and Franco Scarselli. On the Complexity of Neural Network Classifiers: A Comparison Between Shallow and Deep Architectures. *IEEE Transactions on Neural Networks and Learning Systems*, 25(8):1553–1565, 2014.
- [10] Alberto Bietti and Francis Bach. Deep Equals Shallow for ReLU Networks in Kernel Regimes. In *International Conference on Learning Representations (ICLR)*, 2021.
- [11] Valentina Cammarota, Domenico Marinucci, Michele Salvi, and Stefano Vigogna. A quantitative functional central limit theorem for shallow neural networks. *Mod. Stoch. Theory Appl.*, 11(1):85–108, 2024.
- [12] Cristina Campi and Alberto Stefano Tagliafico. Artificial intelligence and prescription of antibiotic therapy: present and future. *Expert Review of Anti-infective Therapy*, 19(1):27–35, 2021.
- [13] Dan Cheng and Armin Schwartzman. Expected number and height distribution of critical points of smooth isotropic Gaussian random fields. *Bernoulli*, 24(4B):3422–3446, 2018.
- [14] Lénaïc Chizat and Francis Bach. On the global convergence of gradient descent for over-parameterized models using optimal transport. In S. Bengio, H. Wallach, H. Larochelle, K. Grauman, N. Cesa-Bianchi, and R. Garnett, editors, *Advances in Neural Information Processing Systems*, volume 31. Curran Associates, Inc., 2018.
- [15] Amit Daniely, Roy Frostig, and Yoram Singer. Toward Deeper Understanding of Neural Networks: The Power of Initialization and a Dual View on Expressivity. *Advances in Neural Information Processing Systems (NeurIPS)*, 29, 2016.

- [16] Alexander G. de G. Matthews, Jiri Hron, Mark Rowland, Richard E. Turner, and Zoubin Ghahramani. Gaussian Process Behaviour in Wide Deep Neural Networks. *International Conference on Learning Representations (ICLR)*, 2018.
- [17] Simmaco Di Lillo, Domenico Marinucci, Michele Salvi, and Stefano Vigogna. Spectral complexity of deep neural networks. *SIAM J. Math. Data Sci. (in press)*, 2024.
- [18] Simmaco Di Lillo, Domenico Marinucci, Michele Salvi, and Stefano Vigogna. Fractal and regular geometry of deep neural networks. 2025.
- [19] S. Favaro, B. Hanin, D. Marinucci, I. Nourdin, and G. Peccati. Quantitative clts in deep neural networks. *Probab. Theory Related Fields*, pages 1–45, 2025.
- [20] Krzysztof M Gorski, Eric Hivon, Anthony J Banday, Benjamin D Wandelt, Frode K Hansen, Mstvos Reinecke, and Matthia Bartelmann. HEALPix: A Framework for High-Resolution Discretization and Fast Analysis of Data Distributed on the Sphere. *The Astrophysical Journal*, 622(2):759, 2005.
- [21] Alexis Goujon, Arian Etemadi, and Michael Unser. On the number of regions of piecewise linear neural networks. *J. Comput. Appl. Math.*, 441:Paper No. 115667, 22, 2024.
- [22] Boris Hanin. Random neural networks in the infinite width limit as Gaussian processes. *Ann. Appl. Probab.*, 33(6A):4798–4819, 2023.
- [23] Boris Hanin and David Rolnick. Complexity of linear regions in deep networks. In *Proceedings of the 36th International Conference on Machine Learning (ICML)*, volume PMLR 97, pages 2596–2604, 2019.
- [24] Geoffrey et al. Hinton. Deep neural networks for acoustic modeling in speech recognition. *IEEE Signal Processing Magazine*, 29(6):82–97, 2012.
- [25] John Jumper, Richard Evans, Alexander Pritzel, Tim Green, Michael Figurnov, Olaf Ronneberger, Kathryn Tunyasuvunakool, Russ Bates, Augustin Židek, Anna Potapenko, et al. Highly accurate protein structure prediction with alphafold. *nature*, 596(7873):583–589, 2021.
- [26] Alex Krizhevsky, Ilya Sutskever, and Geoffrey E Hinton. Imagenet classification with deep convolutional neural networks. *Communications of the ACM*, 60(6):84–90, 2017.
- [27] Jaehoon Lee, Yasaman Bahri, Roman Novak, Samuel Schoenholz, Jeffrey Pennington, and Jascha Sohl-Dickstein. Deep neural networks as gaussian processes. In *International Conference on Learning Representations (ICLR)*, 2018.
- [28] C. L. Mallows. Latent vectors of random symmetric matrices. *Biometrika*, 48:133–149, 1961.
- [29] Domenico Marinucci and Giovanni Peccati. *Random fields on the sphere*, volume 389 of *London Mathematical Society Lecture Note Series*. Cambridge University Press, Cambridge, 2011. Representation, limit theorems and cosmological applications.
- [30] Domenico Marinucci and Giovanni Peccati. Mean-square continuity on homogeneous spaces of compact groups. *Electron. Commun. Probab.*, 18:no. 37, 10, 2013.

- [31] Guido F Montufar, Razvan Pascanu, Kyunghyun Cho, and Yoshua Bengio. On the Number of Linear Regions of Deep Neural Networks. *Advances in Neural Information Processing Systems (NeurIPS)*, 27, 2014.
- [32] Radford M. Neal. *Bayesian Learning for Neural Networks*. Springer New York, 1996.
- [33] Radford M. Neal. *Priors for Infinite Networks*, pages 29–53. Springer New York, New York, NY, 1996.
- [34] Carl Edward Rasmussen and Christopher K. I. Williams. *Gaussian Processes for Machine Learning*. The MIT Press, 2005.
- [35] Daniela Schenone, Rita Lai, Michele Cea, Federica Rossi, Lorenzo Torri, Bianca Bignotti, Giulia Succio, Stefano Gualco, Alessio Conte, Alida Dominietto, et al. Radiomics and artificial intelligence analysis of ct data for the identification of prognostic features in multiple myeloma. In *Medical Imaging 2020: Computer-Aided Diagnosis*, volume 11314, pages 1011–1017. SPIE, 2020.
- [36] Johannes Schmidt-Hieber. Nonparametric regression using deep neural networks with ReLU activation function. *Ann. Statist.*, 48(4):1875–1897, 2020.
- [37] Shizhao Sun, Wei Chen, Liwei Wang, Xiaoguang Liu, and Tie-Yan Liu. On the Depth of Deep Neural Networks: A Theoretical View. *Proceedings of the Thirtieth AAAI Conference on Artificial Intelligence*, 1(30):2066–2072, 2016.
- [38] Ashish Vaswani et al. Attention is all you need. In *Advances in neural information processing systems*, volume 30, 2017.
- [39] Christopher Williams. Computing with Infinite Networks. *Advances in Neural Information Processing Systems (NeurIPS)*, 9, 1996.
- [40] M. I. Yadrenko. *Spectral theory of random fields*. Translation Series in Mathematics and Engineering. Optimization Software, Inc., Publications Division, New York, 1983. Translated from the Russian.